The build-up of the present-day tropical diversity of tetrapods

Ignacio Quintero, Michael J Landis, Walter Jetz, Hélène Morlon

PNAS RESEARCH ARTICLE | EVOLUTION

The build-up of the present-day tropical diversity of tetrapods

Ignacio Quintero[a,1], Michael J. Landis[b], Walter Jetz[c,d], and Hélène Morlon[a]

Edited by Dolph Schluter, The University of British Columbia, Vancouver, Canada; received December 8, 2022; accepted April 4, 2023

The extraordinary number of species in the tropics when compared to the extra-tropics is probably the most prominent and consistent pattern in biogeography, suggesting that overarching processes regulate this diversity gradient. A major challenge to characterizing which processes are at play relies on quantifying how the frequency and determinants of tropical and extra-tropical speciation, extinction, and dispersal events shaped evolutionary radiations. We address this question by developing and applying spatiotemporal phylogenetic and paleontological models of diversification for tetrapod species incorporating paleoenvironmental variation. Our phylogenetic model results show that area, energy, or species richness did not uniformly affect speciation rates across tetrapods and dispute expectations of a latitudinal gradient in speciation rates. Instead, both neontological and fossil evidence coincide in underscoring the role of extra-tropical extinctions and the outflow of tropical species in shaping biodiversity. These diversification dynamics accurately predict present-day levels of species richness across latitudes and uncover temporal idiosyncrasies but spatial generality across the major tetrapod radiations.

diversification | biodiversity | biogeography | tropics | Bayesian inference

Significance

Explaining the remarkable biodiversity of the tropical biome with respect to the extra-tropics can only be explained by different numbers of speciation, extinction, or dispersal events. Yet, the extent to which each of these fundamental evolutionary processes explains present-day spatial variation in biodiversity remains debated. By developing and applying phylogenetic and paleontological models of biogeographic diversification to tetrapods, we find that rather than higher tropical rates of speciation, lower rates of extinction explain their incredible biodiversity, with concomitant diversity outflow into the extra-tropics. Contrary to hypotheses that postulate temperature, geographic area, or diversity dependence as general determinants of speciation rates, we find that idiosyncratic temporal dynamics are key in explaining this widespread diversity pattern.

The present-day increase in species diversity toward the tropics is one of the most widespread biogeographical patterns, shared by a wide array of taxa, including microorganisms, fungi, insects, plants, and vertebrates (1).

The generality of this diversity gradient across continents and clades suggests that universal spatial and temporal evolutionary processes transcend the idiosyncratic ecologies of different lineages (2, 3). Since differences in species richness result from differences in speciation, dispersal, and extinction events, any mechanisms explaining tropical diversity must ultimately link to variation in these processes (4). Therefore, identifying general explanations demands, first, to assess whether the relative contributions among these evolutionary processes coincide across taxa and, second, to investigate whether the mechanisms behind this variation are shared.

How speciation, dispersal, and extinction cause tropical and extra-tropical species richness to differ has been widely debated. On the one hand, variation in species richness can result from differences in evolutionary rates (3, 5). For instance, the tropics could be characterized by abiotic and biotic conditions favorable to speciation, persistence (including lower extinction rates), and/or higher immigration rates when compared to the extra-tropics (4, 6). On the other hand, an older origin and persistence in the tropical biome could provide more time for species to accumulate, even in the absence of rate differences (3). Studies integrating information from both the recent and deeper past generally supported the "evolutionary rate" hypothesis, with evidence for higher speciation rates in species-rich areas (3). In contrast, several newer studies using recent speciation rates found either no association with richness (7, 8) or markedly higher rates in depauperate areas (associated with higher elevations/latitudes) (9–12), advancing the possibility that tropical relative to extra-tropical speciation rates have changed from past to present (5, 13). Rigorously testing these hypotheses, as well as identifying which factors influence temporal variation in tropical relative to extra-tropical speciation rates, has been hampered by the lack of diversification models that account for spatiotemporal evolutionary dynamics in a changing environment and that test for congruence between neontological and paleontological evidence (14). Time-calibrated phylogenetic trees built from the genetic data of extant taxa contain topological and temporal information that, through models, indirectly informs how speciation operates. Fossil information, on the other hand, remains the only direct evidence of extinction and past species distributions; yet, its incompleteness and fragmentary nature hinder a comprehensive characterization of species relationships and their branching process for most clades (15, 16). Approaches using simulation tools have been useful (17, 18), but these frameworks do not provide inference methods to estimate evolutionary parameters from empirical datasets.

Author contributions: I.Q. and H.M. designed research; I.Q. performed research; I.Q. and M.J.L. contributed new reagents/analytic tools; I.Q. and W.J. analyzed data; and I.Q. and H.M. wrote the paper.

The authors declare no competing interest.

This article is a PNAS Direct Submission.

[1]To whom correspondence may be addressed. Email: ignacioquinterom@gmail.com.

This article contains supporting information online at http://www.pnas.org/lookup/suppl/doi:10.1073/pnas.2220672120/-/DCSupplemental.

Published May 9, 2023.

We first developed a set of phylogenetic models that account for the effect of paleoenvironmental variations and observed as well as unobserved ("hidden") species states on spatial diversification, which we call "ESSE" (*Materials and Methods* and *SI Appendix*). These models take advantage of the information encoded in particular combinations of branch lengths, topologies, and distribution of species across geographical regions. Intuitively, branch lengths inform speciation and extinction rates in different regions, topology informs rate differences across lineages associated or not to distinct geographic distributions, and the particular geographical distribution of species across the phylogenetic tree informs past dispersal and between-area speciation dynamics. ESSE combines this information with paleoenvironmental data in a birth–death Bayesian likelihood framework (*SI Appendix*).

ESSE allows diversification rates to vary in space and time while accounting for environmental fluctuations along with variation beyond the geographical distribution of lineages—for example, in relation to other background ecological attributes of the species. This is achieved through a hidden-states framework (19–21), which allows any given geographic range to have subcategories that undergo different diversification dynamics, even if one does not identify the character that groups lineages in different categories (hence their designation as "hidden"). We explored the latitudinal diversification dynamics behind the build-up of the present-day LDG by combining this model with spatial and phylogenetic information for 32,791 tetrapod taxa, representing most extant mammal, bird, amphibian, and squamate species (*Materials and Methods*). We delineate the tropical biome from the extratropics following a biologically relevant environmental definition based on the Köppen climate classification (22) (Fig. 1*A*) (*Materials and Methods*). This definition captures the high productivity and energy characterizing the tropical biome and avoids complications when using other overly inclusive definitions, such as the 23.4° latitudinal cut-off that lumps contrasting biomes like deserts together with evergreen forests (*SI Appendix*, Fig. S1). Collating range distribution information at the validated *ca.* 110 km resolution for all species (23), we assigned each species as either tropical, extra-tropical, or widespread. Consistent with previous studies, our data display a strong latitudinal gradient in species richness across the four major tetrapod clades (Fig. 1*B*) and concomitant richness

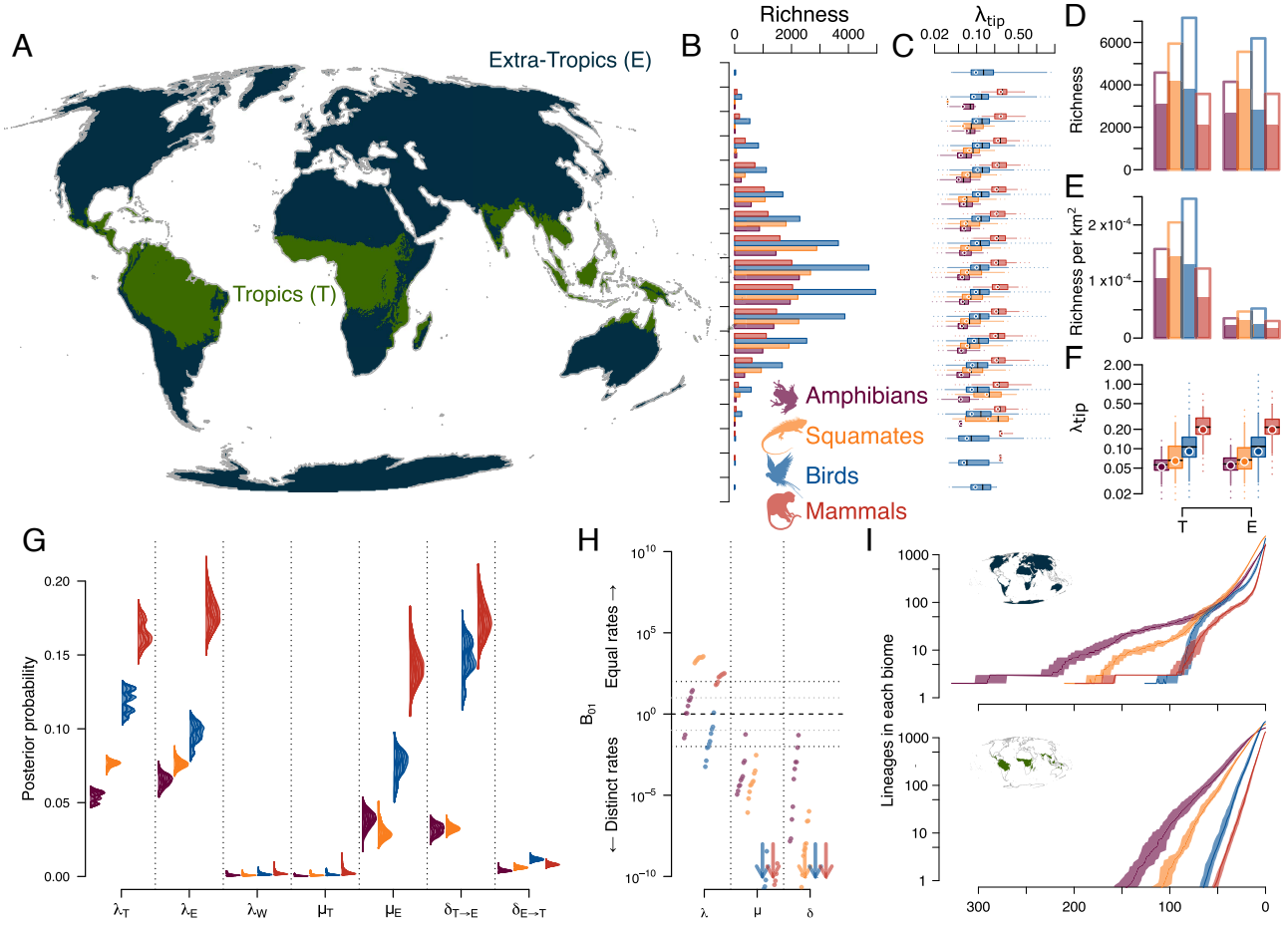

Fig. 1. Latitudinal tetrapod richness and diversification patterns. (*A*) Map of tropical (T) and extra-tropical (E) delimitation. (*B* and *C*) Tetrapod total richness and their present-day speciation rates (λ_{tip}, an average over 10 trees) aggregated by 10° wide latitudinal bands (*D*–*F*) Tetrapod total richness, richness density (per km^2), and present-day speciation rates aggregated by tropical and extratropical regional delimitation (endemics are shown as solid bars). In (*C* and *F*), boxplots show the range (dotted whiskers), 95% quantile (solid whiskers), 50% quantile (box), and absolute median (black line). Circles represent the median weighted by species range size. (*G*) Posterior distributions (with density standardized across all parameters for visualization) across 10 trees for each tetrapod clade for speciation in the tropics (λ_T), extra-tropics (λ_E), and widespread lineages (λ_W), extinction in the two regions (μ_T & μ_E), and dispersal (δ) from the tropics to the extra tropics (T → E) and vice versa (E → T) for model "G", showing no difference in speciation rates between tropical and extra-tropical regions, higher extinction rates in the extra-tropics, and higher dispersal out of than toward the tropics. (*H*) Bayes factors (BF) between "G" models with equal or distinct rates in speciation, extinction, and dispersal (an arrow shows the direction if one or more BFs exceed $> 10^{10}$ in magnitude). (*I*) Lineage through time (LTT) plot for each region and each tetrapod clade as the sum over lineages of the posterior marginal ancestor state probabilities through time (*SI Appendix*).

differences between the tropics and the extra-tropics (Fig. 1*D*), particularly when controlling for their area (Fig. 1*E*). Our analyses used time-calibrated phylogenetic trees with complete species-level sampling for each of the tetrapod clades; species that were nongenetically represented were pruned out but accounted for using region-specific sampling fractions (*Materials and Methods*) to avoid potential inference biases caused by the uncertain placement of these lineages (24).

Elevated Extratropical Extinction Maintains Diversity Gradient

We explored geographic patterns of diversification, first ignoring potential temporal and hidden heterogeneity (model "G"; *Materials and Methods*). In light of inferential concerns about diversification models, we stress that constant rate models (hence the "G" model) are identifiable (25), and we show that biogeographic information strengthens the confidence we can have in extinction rate estimates (*SI Appendix*, *Macroevolutionary Rates*). Contrary to previous studies integrating deep timescales that suggest a negative latitudinal trend with origination rates (26–28) and to studies focusing on recent speciation rates that suggest a positive latitudinal trend (10–12, 29), and matching findings for birds (7, 30), we find that speciation rates have been remarkably similar between the tropics and the extra-tropics across the four major tetrapod radiations, regardless of whether we focus on recent speciation rates (Fig. 1 *C* and *F*) or integrate deeper timescales (Fig. 1 *G* and *H*). Bayesian model selection supported models with equal speciation rates between the tropics and the extra-tropics for most clades (except slightly higher tropical rates in birds, Fig. 1 *G* and *H*). Post hoc association tests of speciation rates at present with either latitudinal bands (Fig. 1*C*) or aggregated tropical or extra-tropical taxa (Fig. 1*F*) were far from significant; *SI Appendix*, Fig. S2).

Our simplest model therefore rejects the hypothesis of higher speciation rates in the tropics relative to the extra-tropics. Similarly, our results do not support the idea that the abundant tropical richness results from more available time for speciation (3): using ancestral states estimation, we find an extra-tropical origin among lineages that survived to the present across all clades followed by more recent colonization of the tropics (Fig. 1*I*), in agreement with recovered crown fossils for amphibians (31), squamates (32), birds (33), and mammals (34). Rather, congruent with previous analyses (26–28, 35), our results suggest that substantially lower extinction rates gave rise to the extraordinary tetrapod richness of the tropics (Fig. 1*G*), with all clades strongly supporting models with region-dependent extinction rates (Fig. 1*H*). Visually, the accumulation of surviving lineages through time shows a clear "pull of the present" signature (36) typical of high extinction in the extra-tropics, while it is almost linear in logarithmic space in the tropics, indicative of very low extinction (Fig. 1*I*). Extra-tropical richness suffers from high extinction rates but is bolstered by a highly supported asymmetrical influx of tropical species (Fig. 1 *G* and *H*). Transitions from the tropics to the extra-tropics result in extra-tropical lineages nested within mostly tropical clades, while the reverse is much less frequent (*SI Appendix*, Figs. S8–S11). This partly agrees with the "Out of the Tropics" hypothesis, wherein tropical clades steadily colonize the extra-tropics over time (6). Similar analyses conducted with a latitudinal cut-off rather than the Köppen classification of the tropics no longer provided such consistent results across vertebrates (*SI Appendix*), suggesting that the Köppen classification provides a more ecologically and evolutionary relevant characterization of the tropics and that our use of this criteria probably explains, at least in part, why some of our results contrast with previous studies (*SI Appendix* for a detailed comparison with previous studies).

Incorporating hidden states to these geographical models (model "G+H") reveals that tropical and extra-tropical lineages each further separate into two intraregional diversification regimes (Fig. 2 *A* and *B* and *Materials and Methods*). These regimes represent rate variation across lineages that all pertain to the tropics, the extra-tropics, or are widespread. For instance, the model reveals that not all tropical lineages undergo the same diversification dynamics but rather that some proportion have significantly higher net diversification rates (those in hidden state 1) than the others (those in hidden state 0) for all clades except amphibians (Fig. 2*A*). Regardless of the hidden state, the tropics act as a "source," accumulating species steadily with a net outflow of species toward the extra-tropics. In contrast, the extra-tropics either experience more extinction than speciation events, acting as a "sink" (lineages in hidden state 0), or experience more speciation than extinction events (lineages in hidden state 1) (Fig. 2 *A* and *B*). Among the high influx of lineages toward the extra-tropics, our model detects which lineages became evolutionarily successful and which were more prone to rapid extinction. The lineages with high recent extra-tropical speciation rates correspond to those in hidden state 1, with a deep-time net diversification rate comparable to that in the tropics (Fig. 2 *C* and *D*; strongly supported associations, Dataset S2), challenging the idea that these fast speciating lineages are ephemeral on account of their high extinction rates (9, 12). These lineages also have a present-day speciation rate that does not exceed tropical rates (Figs. 1*F* and 2*A*), undermining the possibility that even if these high present-day speciation rates hold in the future, the extra-tropics could eventually achieve comparable diversity to the tropics (10).

Environmental Change Elicits Idiosyncratic Diversification Responses Across Clades

To test the hypothesis that the relation of tropical to extra-tropical speciation rates has changed from past to present and to identify factors that have potentially influenced this temporal variation, we consider a series of ecologically important variables that have changed through time and are thought to influence speciation rates. Total terrestrial tropical and extra-tropical areas have fluctuated dramatically across geological history (37), and speciation rates are predicted to be higher in large geographical regions by offering more opportunities of within-area population divergence and by supporting species with wider ranges (38, 39). Similarly, area expansion can increase speciation rates as lineages track their abiotic preferences across space, inducing geographical range shifts and fragmentation (40). Temperatures have also fluctuated across geological history (41), and warmer environments are expected to enhance speciation by being more productive environments that support higher population numbers and by accelerating evolutionary speed at the molecular level, offering more opportunities for population differentiation (2, 42). Speciation rates might also increase with the rate of temperature change, through climate-driven dispersal and vicariance events that isolate populations (40). Lastly, latitudinal differences in resource availability could either constrain speciation rates under a negative diversity-dependence scenario (43) or promote speciation by increasing the probability of divergence either by interspecific competition or by lowering average population numbers, and by generating higher

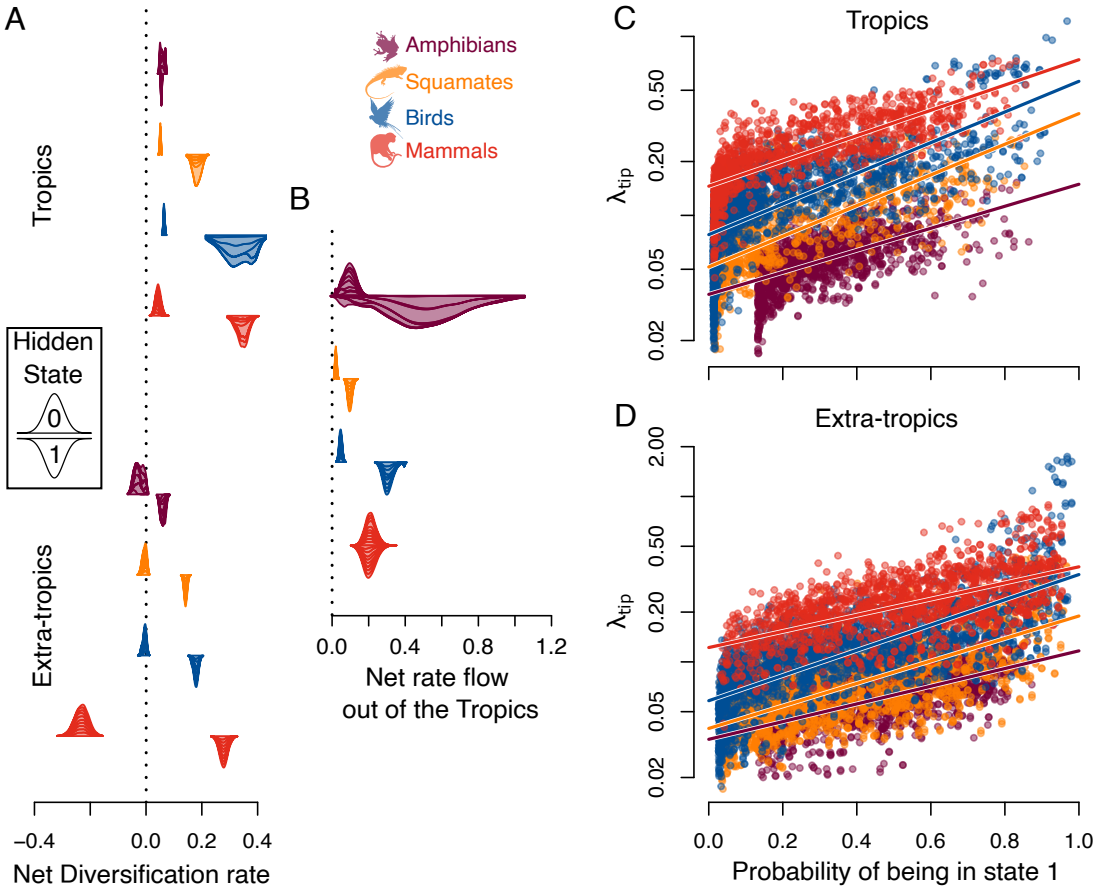

Fig. 2. Heterogeneity in diversification rates within regions. Results of the "G+H" model, which includes two hidden states (0 and 1) that represent two rate categories within each of the geographical regions that are not related to any observed character. (*A* and *B*) Posterior distributions (with density standardized across all parameters for visualization) across 10 trees for each tetrapod clade for (*A*) net diversification rates ($\lambda - \mu$) in the tropics (*Top*) and extra-tropics (*Bottom*) and for (*B*) net rate flow out of the Tropics ($\delta_{(T\to E)} - \delta_{(E\to T)}$), for the two hidden states (0: up-facing and 1: down-facing). Lineages in hidden state 1 have similar net diversification rates in the tropics and extra-tropics, and higher net diversification rates than those in hidden state 0 in both the tropics and the extra-tropics. In the extra-tropics, lineages in state 0 have a negative net diversification rate. (*C* and *D*) Tip-speciation rate (λ_{tip}) versus corresponding marginal posterior tip probabilities of being in hidden state 1 for (*C*) tropical and (*D*) extra-tropical species. Lineages with a high present-day speciation rate tend to be in the state with higher deep-time net-diversification rates (i.e., state 1). Clade colors as in Fig. 1.

community complexity through a "diversity begets diversity" scenario (44).

We tested if regional species richness is explained by speciation rates controlled by habitat-specific area and its rate of change, temperature and its rate of change, or diversity-dependence using a time-varying spatiotemporal model of lineage speciation, extinction, and dispersal (model "G+E+H"; *Materials and Methods*). These models are identifiable, as we allow rate heterogeneity across lineages and constrain the functional form of the rate dependencies, but provide results that rely on the assumed particular functional form linking rate parameters with environmental dependencies (*SI Appendix*).

Our process-based approach allows to better evaluate ecological theories underlying richness variation by integrating deep-time environmental covariates and spatial diversification dynamics rather than by correlating present-day covariates with extant biodiversity. We estimated tropical and extra-tropical terrestrial areas by merging reconstructed Köppen biomes and Digital Elevation Models to reconstruct worldwide tropical and extra-tropical regions every 5 My for the past 540 Mya (45, 46) (*Materials and Methods*, Fig. 3 *A* and *B*, and Movie S1). Consistent with previous literature, we find that the tropical biome was larger at the beginning of the Cenozoic than today, and present at high latitudes (i.e., 45° to 60°) (47, 48), but that the corresponding (large) latitudinal band equated with "the tropics" was far from fully tropical; instead, it contained a vast highly arid region in between [(49), Movie S1]. We used these reconstructions as region-specific covariates of tropical and extra-tropical speciation rates, respectively. Similarly, we compiled global temperature data for the past 526 Mya (Fig. 3*D*) and allowed for different associations between tropical and extra-tropical speciation rates with temperature. We used a region-specific exponential relationship of speciation rate with time to approximate the effect of diversity-dependence (50) (*Materials and Methods*). We assumed region-specific, but time-constant, extinction rates as our model validation confirmed previously noted difficulties in recovering time-varying extinction dynamics from phylogenies of present-day species (51, 52). We show, however, that under simulated scenarios using empirical extinction rate curves, we are able to recover the pertinent time-averaged extinction rates between regions (*SI Appendix*).

Intriguingly, while we find that the correspondence across tetrapods in geographic diversification and dispersal patterns holds after incorporating temporal dynamics, the temporal dynamics themselves are highly idiosyncratic (model "G+E+H," Fig. 3*F* and *SI Appendix*, Figs. S3–S5). While time-averaged rates

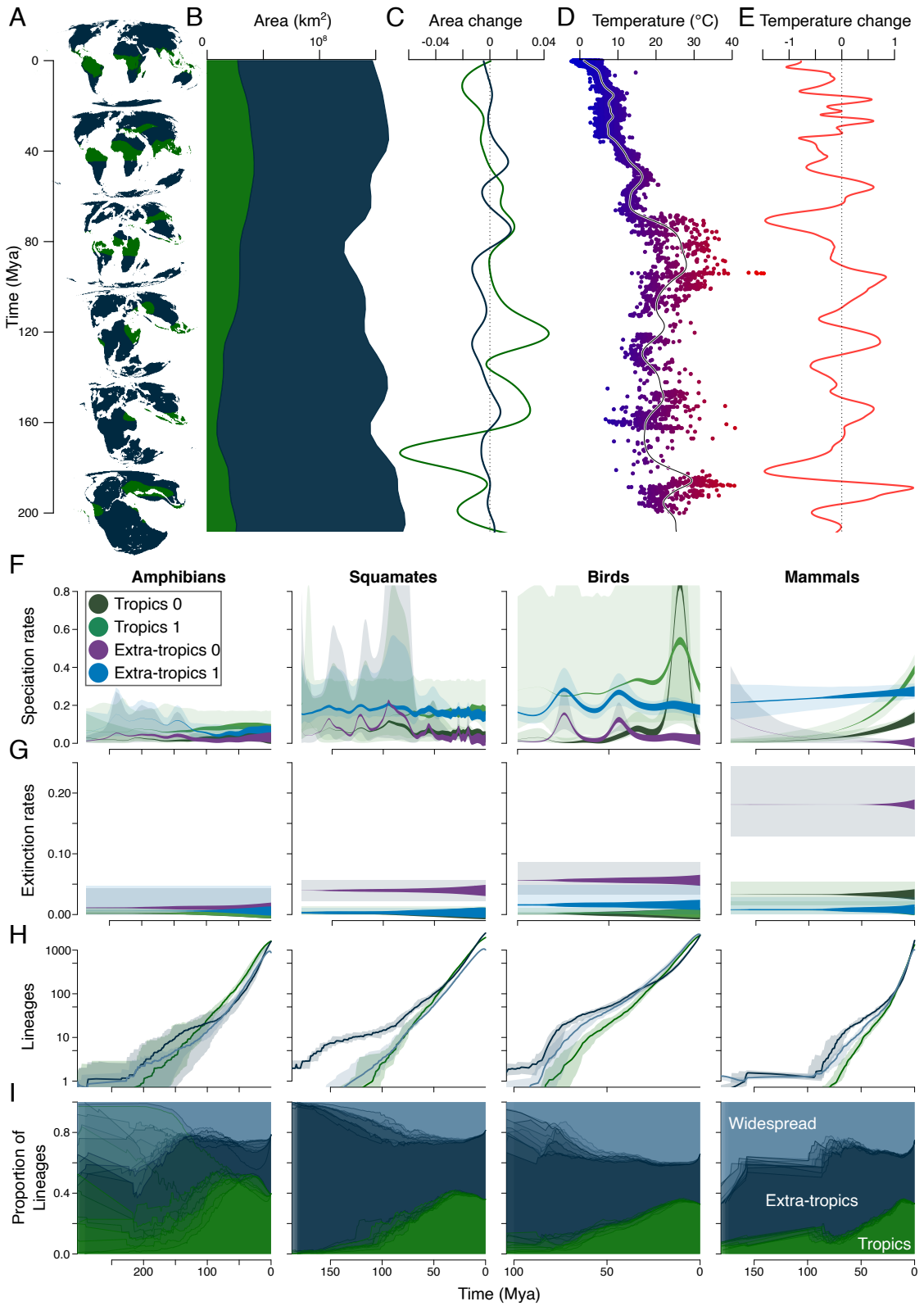

Fig. 3. Results of the "G+E+H" model, which includes two hidden states (0 and 1) and allows for paleoenvironmental data to shape speciation rates. (*A*) Maps every 40 My of tropical and extra-tropical terrestrial area. (*B*) Tropical and extra-tropical area reconstruction, (*C*) their respective change (logarithmic derivative with respect to time), (*D*) temperature, and (*E*) its rate of change for the last 200 My. (*F* and *G*) "G+E+H" rate estimates in the tropics and the extra-tropics for each of the two hidden states (0 and 1) according to the best-selected paleoenvironmental models with time-varying speciation (*F*) and time-constant extinction (*G*) (amphibians: area "A(t)" and exponential time dependency "ETD", reptiles: temperature "T(t)" and "A(t)," birds: "A'(t)," mammals "EDT"). 95% HPD uncertainty is displayed as background shade using model averaging by weighting each tree and parameter contributions by their posterior probability. The thickness of the line corresponds to the state-specific reconstructed number of lineages (in natural logarithm) that survived to the present. (*H*) Region-specific LTT aggregated from ancestral posterior probabilities of being tropical, extra-tropical, or widespread (*SI Appendix*). (*I*) LTT proportions in each state across time (lines correspond to the 10 pseudo-posterior trees).

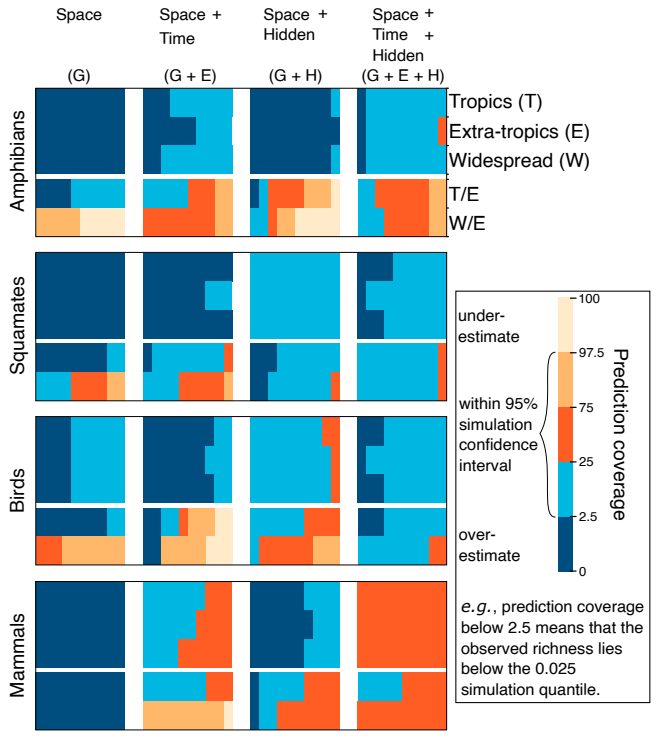

Fig. 4. Goodness of fit of diversification models. Prediction coverage from the richness probability distributions for diversification models, in increasing complexity: Space = geographic dependence (G), Time = environmental dependence (E), and Hidden = hidden states (H). Prediction coverage is defined as the model-predicted quantile of species richness using simulations that contains the empirical measurement of true species richness. For each clade (rows), for each model (column), a subrow consists of results for each of the 10 trees in sequence (subcolumns) and represents, in order, tropical, extra-tropical, and widespread richness and proportion of tropical/extra-tropical and widespread/extra-tropical.

show similar patterns as the constant rate models (i.e., to models "G" & "G+H"; *SI Appendix*, Figs. S4 and S5), we find support for distinct nonlinear speciation rate dynamics where the tropical and extra-tropical rates exceeded each other at different times in the past (Fig. 3*F*). For amphibians and squamates, different time dependencies on speciation were selected for different posterior trees, indicating that while speciation has not been constant, the data do not tell us which time-dependent hypothesis is the most likely (Dataset S4). Model-averaged rate curves for these clades, however, show that tropical and extra-tropical speciation rates both decline slightly in the recent past. Bird speciation rate dynamics most closely responded to the rate of area-change through time, with lineages experiencing higher speciation rates when area contracts rapidly in the tropics and when area expands rapidly in the extra-tropics (Fig. 3*F* and *SI Appendix*, Fig. S5). For mammals, diversity-dependent speciation rates were strongly supported, but with opposite effects for the two regions. In the tropics, mammal diversity begets diversity regardless of species hidden state; in the less productive extra-tropics, diversity either has no strong effect and net diversification rates are positive (hidden state 1) or diversity impedes diversity, which in combination with high extinction rates, induces the "sink" regime (hidden state 0; Fig. 3 *F* and *G*).

To test our model's ability to predict present-day tetrapod latitudinal diversity patterns, we performed forward-time simulations under our fitted models to compare predicted and observed tropical and extra-tropical species richness (*Materials and Methods* and *SI Appendix*, Fig. S11). We found that except for birds, models without within-region rate heterogeneity in the diversification process (without hidden states) or that ignore temporal speciation dynamics consistently overestimate the number of species at present across regions and overpredict the ratio of widespread to extra-tropical lineages (Fig. 4). Instead, models with temporal and geographical dependencies, coupled with within-region rate heterogeneity, accurately predict the observed richness in number of tropical, extra-tropical, and widespread species for all clades (Fig. 4).

Elevated Extratropical Extinction Reflected in Fossil Data

For a comprehensive assessment of these spatial diversification dynamics, we applied an analogous biogeographic model that uses fossil occurrences instead of phylogenetic trees, "DES," and that accounts for several sources of uncertainty such as temporal and spatial sampling and preservation (16). While existing paleontological biogeographic models do not infer speciation rate dynamics (in "DES" the processes of origination and range inheritance are ignored (16)), they provide direct observations of past extinction and dispersal events and relax the assumption of constant extinction rates through time for each area, evaluating the robustness of our phylogenetic models results. We focused on mammal dynamics during the Cenozoic since they have by far the best paleontological record of a terrestrial clade across tropical and extra-tropical regions (37, 53) and carefully vetted spatial fossil occurrence data at the genus level, following standard

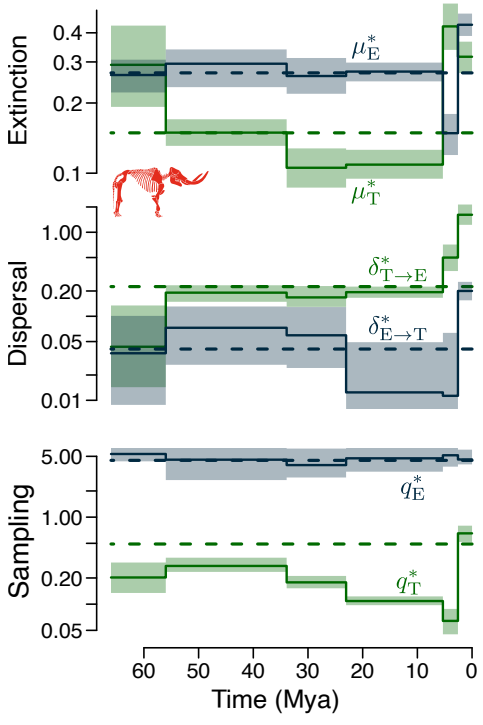

Fig. 5. Spatiotemporal diversification dynamics in mammal fossil record. Results from Cenozoic fossil biogeographic analyses at the genus level for tropics in green and extra-tropics in blue. Dashed horizontal lines reflect results from time-constant models while solid skylines show time-heterogeneous rates following stratigraphic periods (shading reflects 95% HPD intervals). *Top:* fossil extinction rates for the tropics (μ^*_T) and the extra-tropics (μ^*_E). *Middle:* fossil dispersal rates from the tropics to the extra-tropics ($\delta^*_{T\to E}$) and vice-versa ($\delta^*_{E\to T}$). *Bottom:* fossil sampling rates for the tropics (q^*_T) and the extra-tropics (q^*_E) (Mastodon silhouette credits: Becky Barnes' North Dakota Geological Survey).

paleontological practice (*Materials and Methods*). We then allocated fossil occurrences using their timing and paleocoordinates to the corresponding spatiotemporal reconstructions of global tropical and extra-tropical regions.

Remarkably, our paleontological results concur with those from our phylogenetic methods in that the extra-tropical region experienced higher extinction rates together with higher immigration of tropical diversity, regardless of assumptions of temporal rate constancy or heterogeneity across separate stratigraphic periods, while accounting for temporal and spatial fossil sampling differences (Fig. 5). While the use of different taxonomic resolutions as well as different taxonomic concepts (54, 55) make phylogenetic and fossil-based model rates not directly comparable, they highlight the relative region-specific rate differences in extinction and dispersal (16). Our results using phylogenetic information are also congruent with other results based on paleontological evidence (37, 56), highlighting the utility of combining biogeographic and birth–death information for capturing past diversification dynamics.

Conclusions

Both our phylogenetic and paleontological results emphasize the key role that extra-tropical extinction played in shaping present-day latitudinal diversity patterns. They reject the hypotheses of an older, larger, or more speciation-prone tropical biome leading to current richness. Instead, they support the hypothesis that surviving diversity accumulated in the tropics under low extinction, dispersed out of the tropics, and suffered from frequent extinctions in the extra-tropics. These frequent extinctions did not affect species equally: Some extra-tropical lineages accumulated species just as fast as those in the tropics, while others experienced negative diversification rates. These differences likely reflect species-specific traits that offer varied resilience to cope with the somewhat harsher environments of the extra-tropics, although this remains to be tested. Our results show an extraordinary correspondence in region-dependent diversification and dispersal patterns across the four tetrapod clades, despite each clade's idiosyncratic responses to paleoenvironmental dynamics. Markedly distinctive ecologies across clades underlie multiple routes to an overarching latitudinal variation in geographical diversification that brought about one of the most striking diversity patterns on our planet.

Materials and Methods

Tropical and Extra-Tropical Definition. We use the Köppen biome classification (90) to define tropicality and extra-tropicality. The Köppen biome classification is based on temperature and precipitation and their seasonal components and delimits evolutionary and ecologically meaningful regions (22). While there are several ways to define the tropics and extra-tropics (e.g., 23.4° south and north latitudes, *SI Appendix*), we adopt our classification for two main reasons. Firstmost, climatic variables are the major determinants of species distributions, providing a biologically meaningful spatial delimitation when explaining species richness patterns. Climatic variables are strongly correlated with latitude, but local topographical and regional features can distort the expectation of a tropical biome, even at low latitudes (*SI Appendix* for a comparison with 23.4° latitudinal delimitation). Because computational limits do not allow a finer regionalization across biomes, we define the "extra-tropics" as the nontropical biomes. While the extra-tropic merges different biomes (just as a 23.4° to 23.4° latitudes classification does, *SI Appendix*, Fig. S1), they share a lower productivity and a much lower species density than the tropics. Second, our delimitation matches the spatial paleoclimatic reconstruction (below) based also on the Köppen classification scheme to estimate tropical and extra-tropical area through deep-time (*SI Appendix*).

For present-day spatial tropical delimitation, we extracted the raster data at 1-km resolution from the study by Beck et al. (22), who divided the terrestrial globe into five main classes and thirty subtypes. We aggregated all tropical subtypes (i.e., "Af":Tropical Rainforest, "Am":Tropical Monsoon, "Aw":Tropical Savannah) to define a tropical biome and aggregated the remaining subtypes as extra-tropical (22). Effectively, this delineates the tropics as a region where the Mean Air Temperature of the coldest month is above 18 °C and that has high Mean Annual Precipitation (see ref. 22 for details). We then reprojected the raster data into the Mollweide projection, which preserves equal-area proportions across the globe (Fig. 1*A*).

Terrestrial Vertebrate Data. We aggregated phylogenetic and spatial information for all extant species of amphibians, squamates, birds, and mammals. Phylogenetic data for amphibians were obtained from ref. 57 (7,238 total species, 4,061 genetically represented), for squamates from ref. 58 (9,755 total species, 5,415 genetically represented), for birds from ref. 7 (9,993 total species, 6,670 genetically represented), and for mammals from ref. 59 (5,806 total species, 4,001 genetically represented). We excluded the Tuatara species (*Sphenodon punctatus*) from the phylogeny in ref. 58 because Tuatara is not a squamate. We excluded pelagic-breeding mammal species (i.e., Cetaceans, 105 species) since terrestrial covariates are unsuited for assessing their evolutionary history. Across the other vertebrate groups here considered, only one species of sea snake is pelagic, *Hydrophis platurus* (60), while the other, paraphyletic, sea snakes rely on land or close proximity to low salinity waters associated with terrestrial habitats to breed, so we did not exclude them (61). We excluded 13 species of domestic mammal animals for they have mostly responded to human selection and have unusual human-mediated cosmopolitan biogeographic distributions, which might conflate the natural diversification dynamics but included many human-induced recent extinct species (103 spp. that went extinct in the last 500 y). For each clade, we randomly sampled 10 trees from the posterior to accommodate phylogenetic uncertainty in posterior analyses.

Spatial information was carefully vetted and collated to match the taxonomy of the phylogenetic trees, obtained from VertLife project (vertlife.org) in association with Map of Life (mol.org). Breeding range distribution data for birds followed (7). Mammal and amphibian distribution data were based on IUCN data (62) that were modified to match taxonomically with the respective phylogenies. For squamates, data were based on ref. 63 with careful taxonomic matching with the phylogenetic tree. We performed a literature search to assign those species without spatial distribution information as either tropical, extra-tropical, or widespread (species-specific references can be found in Dataset S1). For mammals, we note that we included recently extinct species (in the last 500 y) represented in the tree, which have been sampled from few locations and might not be representative of the whole range (Dataset S1).

To encode species ranges as tropical, extra-tropical, or widespread, we used expert breeding ranges defined for 360 equal area grid cells (110-km grain size) since they have been previously validated to have minimum (<5 to 10%) false presences at such spatial grain (23). We then counted the number of tropical and extra-tropical 1-km cells from the binary Köppen layer inside each species range to assign them as tropical, extra-tropical, or widespread using 4 different "cut-offs". As the most stringent cut-off, we required at least 20% of the range to pertain to either the tropical and extra-tropical area to be assigned that area; then, we used 15%, 10%, and 5% in decreasing order of regional exclusivity (64). Complementary analyses showed that the different cut-offs did not significantly impact our primary findings concerning diversification patterns (*SI Appendix*, Fig. S6), and thus, we carried on using only the most stringent cut-off of 20%, which is conservative in allocating tropical and extra-tropical taxa. Briefly, the least conservative cut-off of 5% produces a higher proportion of widespread lineages (concomitant with fewer endemics), which, in turn, increases dispersal rates from the tropics to the extra-tropics and decreases in situ speciation rates in the extra-tropics compared to the 20% cutoff (*SI Appendix*, Fig. S6).

After allocating all extant species of amphibians, squamates, birds, and mammals as tropical, extra-tropical, or widespread, we pruned all species from each phylogeny that were not placed using genetic data and then estimated the sampled fraction for each of those states in the resulting trees. The resulting sampling fractions for the tropics (T), extra-tropics (E), and widespread (W) taxa for the 20% cut-off are for amphibians (T = 0.520, E = 0.594, W = 0.585), for

squamates (T = 0.464, E = 0.648, W = 0.569), for birds (T = 0.574, E = 0.775, W = 0.681), and for mammals (T = 0.612, E = 0.767, W = 0.686), respectively, and showcasing the overall genetic undersampling of the tropics. Our main results used only genetically sampled species to avoid biases in assuming an artificial geographic evolutionary history resulting from any unnatural placement of nongenetically sampled species (24). Given biome conservatism, random placement of nongenetically sampled species should yield more sister taxa with mismatched biome states than one would expect with correct species placements. In any case, we compared our results using all species, obtaining similar results overall but, as expected, with inflated rates of transitions and between-region speciation (*SI Appendix*, Fig. S6). Species regional allocation (using Köppen and latitudinal classification at the 5%, 10%, 15%, and 20% cut-offs) and the trees we used are found in *SI Appendix*.

Tip Speciation Rates Analyses. To estimate tip speciation rates (i.e., speciation rates at present) for each of the four tetrapod clades, for each of the 10 posterior tree samples, we made inference under the ClaDS model (65) using the data augmentation implementation (66). ClaDS assumes speciation rates are constant within each branch of the tree but are inherited with a shift at speciation, thereby providing branch-specific speciation rates. We ran ClaDS using ambiguous priors on the hyperparameters under a constant turnover model for as many iterations as necessary for the Gelman–Rubin statistic (67) to become lower than 1.05 (the default stopping behavior). We then retrieved the present-day speciation rates for each species by taking the maximum a posteriori estimate for each of the 10 phylogenetic trees for each clade.

To test for a latitudinal effect on speciation rates, we used Bayesian linear models corrected for phylogenetic nonindependence using the "MCMCglmm" (68) package in R (69). We first calculated the latitudinal centroid for all species and explored the effect of absolute latitude centroid on the natural logarithm of tip-speciation rates. We then estimated if there was a difference between tropical and extra-tropical biomes in speciation rates. We ran the analyses for each clade and for each tree for 500k MCMC iterations with a 2k burn-in using ambiguous inverse Wishart priors (expected covariance of 1 and $\nu = 2e - 4$) and visually checked for good mixing and convergence.

Paleoenvironment Reconstructions. To quantify the tropical and extra-tropical terrestrial area through time, we used plaeoclimatic and paleoelevational reconstructions that date as far as 540 Mya with a sampling frequency of every 5 Myrs. Paleo-Digital Elevation Models, "PaleoDEMs", were obtained at a 1° resolution from ref. 45. Similarly, for the same time stamps, we used Köppen classification reconstructions from ref. 46 with corresponding 5 Myr interval maps. These reconstructions are based solely on the five main climate classes (i.e., tropical, arid, warm temperate, cool temperate, and polar), which we divided into tropical and extra-tropical (*SI Appendix*). We reprojected these data into the Mollweide projection and intersected terrestrial land, by using only grid cells above sea level, with either tropical and extratropical classification. Finally, we counted the number of grid cells and multiplied by their area to obtain tropical and extra-tropical area every 5 Myrs from the present back to 540 Mya (Fig. 3 and Video S1). All spatial analyses were conducted with gdal (70) and raster package (71) for R (69). We used deep-time global temperature estimates for the Phanerozoic eon from ref. 72. We smoothed the tropical and extra-tropical area and temperature curves using spline smoothing in R using the "pspline" package (69, 73). For temperature ("T(t)") and region-specific area ("A(t)"), we also estimated their rates of change by taking the derivative from the smoothed curves ("T′(t)" and "A′(t)," respectively (Fig. 3 *C* and *E*). These curves were used as environmental covariates affecting time-varying rates of speciation in the ESSE model (below) and are found in *SI Appendix*. To test diversity dependence, we simply used time as the covariate, which results in testing an exponential time dependency (noted "ETD") (50).

Effect of Environment on Diversification Across Space. We expand on current state-dependent speciation and extinction (SSE) models to allow for environmental dependency. We call these sets of models Environmental SSE models, "ESSE". In general, SSE models enable inference on distinct rates for speciation, extinction, and state transitions depending on a discrete state and, yet, for a given state, remain constant through time. Cantalapiedra et al. (74) enabled environmental dependency on speciation rates for MuSSE within a likelihood framework (75), using a different mathematical formulation than the one presented here. We generalize by allowing rates of speciation, extinction, and state transitions to depend on discrete states, including hidden states as in "HiSSE" (19), as well as time-varying covariates $\boldsymbol{z}(t)$, whose effect on rates of speciation, extinction, and state transitions is regulated by parameters β within a Bayesian framework.

Our ESSE model elaborates on the Geographic State Dependent Speciation and Extinction ("GeoSSE") model introduced by ref. 76 and later enhanced by ref. 20 to include Hidden States ("GeoHiSSE"). Hidden states in SSE models have been validated when using a combination of observed and missing states (19, 20) and when using only nonobserved states (21, 77). In GeoHiSSE models, each area i and hidden state h has a rate of speciation ($\lambda_{i,h}$) and extinction ($\mu_{i,h}$), each pair of areas i, j and hidden state h have a rate of dispersal (from $i \rightarrow j$, $\delta_{i,j,h}$ & from $j \rightarrow i$, $\delta_{j,i,h}$) and a rate of between-region (i.e., allopatric) speciation ($\lambda_{i,j,h}$), and a transition rate between hidden states h and l ($\phi_{h,l}$; details in *SI Appendix*). ESSE also adapts ideas from the Feature-Informed GeoSSE ("FIG") model (78) by allowing per-area speciation, extinction, or dispersal rates to vary according to time-dependent state-specific covariates, such as paleobiome size or temperature. While we enable here the most general model, in practice, some parameters have to be constrained (below), resulting in simpler models, to perform effective inference. Let $z_i(t)$ be a vector of length p at time t of some arbitrary functions that change through time (e.g., regional area through time), specific to lineages in area i, and let $\beta_{\gamma,i,h}$ be a $p \times 1$ matrix of the parameters regulating the effect of $z_i(t)$ on rate $\gamma_{i,h}$ experienced by a lineage in area i with hidden state h. We then allow per-area speciation (λ) and extinction (μ) rates, $\gamma_{i,h} = \{\lambda_{i,h}, \mu_{i,h}\}$, to depend on $z_i(t)$ multiplicatively, such that $\gamma_{i,h}(t) = \gamma_{i,h} \exp\left(z_i(t)'\beta_{\gamma,i,h}\right)$, where $\gamma_{i,h}$ is a baseline constant rate not influenced by time-varying covariates. For a covariate effect on dispersal rates, δ, the covariates affect pairwise area rates, such that $\delta_{i,j,h}(t) = \delta_{i,j,h} \exp\left(z_{i,j}(t)'\beta_{\delta,i,j,h}\right)$, where $\delta_{i,j,h}$ is the colonization rate from area i to area j under hidden state h. Beyond environmental diversification models (51), an exponential multiplicative dependency of rates has been used widely and effectively in medical research on survival analyses to estimate effect of covariates on rates i.e., hazard ratios in the Cox model (79), and we show that it provides adequate absolute model fit (below). The likelihood calculations, Bayesian inference, validation, and the estimation of posterior marginal probabilities for ancestral states, are detailed in (*SI Appendix*, Fig. S7).

Implementation. These methods are available as part of the "Tapestree" (80) and "PANDA" (81) packages for Julia > v1.5 (82). The likelihood calculations were programmed using the "DifferentialEquations.jl" package (83) to perform numerical integration of the ODE functions. We use "meta-programming" techniques to produce specialized code at run time given the model specified by the user to attain higher performance. Particularly, we are able to generate state-specific functions, including the ODE function to be passed to the numerical solver. Our ESSE implementation allows for different combinations of models that can be specified: i) designation of rate dependency (i.e., if speciation, extinction, and/or dispersal rates are specified as dependent on a series of time-varying covariates); and ii) number of covariates per covariate-dependent rate (i.e., p); iii) number of states (i.e., $|K|$); and iv) number of hidden states (i.e., $|H|$). Furthermore, any number of logical constraints between parameters, or fixing of parameters to a determined real value can be specified. Because these models have a very rugged posterior and inference algorithms can get stuck in local optima, including the default Bayesian algorithm of "GeoSSE" on the "diversitree" package (75) for R (69) (*SI Appendix*, Fig. S12), we developed parallel Metropolis-coupled MCMC with temperature tempering to enhance the chances of finding the more likely combination of parameters (84).

Empirical Inference. For each tetrapod clade, we performed inference on each of 10 phylogenetic trees sampled from the posterior to accommodate phylogenetic uncertainty. We were restricted to only 10 trees given the computation cost in time and number of processors needed (below). To gain a comprehensive picture of the diversification dynamics and aid in interpretation,

we fitted progressively more complex geographical diversification models. First, we ran a geographically dependent model with time-constant rates and without hidden states ("G"; i.e., our own implementation of "GeoSSE"). We compared our results to using a purely latitudinal tropical delimitation (*SI Appendix*, Fig. S13). The second model included environment-dependent speciation rates but still no hidden states ("G+E"). The third model included two hidden states but no environment-dependent rates ("G+H"; i.e., our own implementation of "GeoHiSSE"). The fourth model included both environment-dependent speciation rates and two hidden states ("G+E+H"). While computational limitations made the addition of a finer regionalization of the world into, say, more biomes or the inclusion of more hidden states unfeasible (*SI Appendix*), we find that at least with this complexity, absolute model fit was adequate to predict observed richness patterns (below). For all models, all parameters varied freely (including transition rates among hidden states, in contrast to "GeoHiSSE"), except for constraining the local extinction rate to be equal to the global extinction rate (*SI Appendix*). We used uninformative exponential priors, $\mathrm{Exp}(0.1)$, for all rate parameters and uninformative Gaussian priors for β, $\mathrm{N}(0, 10)$. This model fitting procedure resulted in the examination of 1 "G" diversification scenario, 5 "G+E" scenarios (with area, temperature, their derivatives, and time as covariates), 1 "G+H" scenario, and 5 "G+E+H" scenarios, for a total of 12 diversification scenarios. We ran each of these on 10 posterior trees for each of 4 tetrapod clades, that is, a total of $12 \times 10 \times 4 = 480$ model fits (aside from simulations and runs to appraise sources of bias; *SI Appendix*, Figs. S6 and S7). Moreover, each model fit consisted in 3 Metropolis-coupled Markov chain Monte Carlo (MC3) chains and $\Delta T > 0.5$ to guarantee as much as possible good convergence behavior over the complex posterior surface, requiring 1,440 computing nodes.

We then performed model comparison using Bayes factors and selected the best-performing models across scenarios (*SI Appendix*). Finally, we further tested absolute model fit by performing simulations from the best-performing models, as follows.

Bayesian Model Adequacy. We evaluate the adequacy of our best-fitting models by testing their power to predict current latitudinal patterns of species richness across tetrapods. Performing posterior predictive tests examines the capacity of a model to predict the observed data and thus if the model adequately describes key data features, that is, it provides a measure of absolute model fit (85, 86). We aim to compare the observed numbers of tropical, extra-tropical, and widespread species to regional richness probability distributions (RPDs) under our four models: G, G+E, G+H, and G+E+H. Because no analytical solution is available for RPDs under these models, and approximating them entirely with simulations resulted in a nonnegligible fraction of cases exceeding the guard of a maximum of 100k total simulated lineages put in the first place to avoid high computational costs, we used a combination of simulations and parametric approximation of the RPD (*SI Appendix*). We estimated the RPD quantiles per tree, per clade, per region and compare them to the empirical estimates. These numerical solutions are included in the software package.

Biogeographic Fossil Analyses of Mammals. To test for congruent historical evolutionary dynamics from both neontological and paleontological evidence, a clade with both well-known fossil record and complete phylogenetic tree is required. We thus focused on Mammals, which, during the Cenozoic, remain the best sampled major tetrapod radiation in the fossil record (37, 53). We downloaded Mammal fossil occurrence data from the Paleobiology Database (PBDB) on July 2022 (87) for all mammals (i.e., "Class" = "Mammalia") excluding Cetaceans, since we work with terrestrial regions. We first vetted the resulting database by removing occurrences with a reported interval larger than 5 My for occurrences younger than 23.04 Mya, larger than 10 My for occurrences younger than 66.02 Mya, and larger than 15 My for all other occurrences. We then discarded all occurrences without a defined genus classification. Following common practice in paleontology, we performed all subsequent analyses at the genus level, which are less contingent on preservation and sampling biases, correlate well with species-level patterns of diversity, and better reflect underlying diversification patterns (88, 89). To incorporate dating uncertainties, we produced 10 randomized datasets by sampling uniformly within the temporal range of each fossil occurrence (16). We then used the tropical and extra-tropical paleoenvironmental reconstructions to assign each fossil occurrence as tropical or extra-tropical according to their timing and paleocoordinates and allowing a buffer diameter of 100 km, following the grain from the spatial reconstructions. This resulted in 74,722 fossil occurrences allocated across the two regions, including occurrences older than the Cenozoic (Dataset S5). While we only considered the Cenozoic, including these occurrences is important for better estimation of sampling rates across genera that survived the K-Pg mass extinction.

We then used the dispersal–extinction–sampling ("DES") model (16), which uses MCMC to estimate per-area dispersal, extinction, and sampling rates. The sampling rate includes the fossilization and preservation of an organism, its modern recovery, and its taxonomic identification. DES has been shown to outperform other methodologies that infer past diversification dynamics (16). We ran two separate models on the same dataset: First, we constrained dispersal and extinction rates to be constant across the Cenozoic for each area, and then, we allowed for time-heterogeneity by allowing rates to change according to stratigraphic ranges. For both models, we allowed time and taxonomic heterogeneous sampling rates. We ran each of the 10 replicates for 2×10^5 iterations and monitored convergence to then remove 10^5 iterations as burn-in. For the final results, we combined the 10 replicates, which showed very little variation among them.

SI Appendix can be found in https://doi.org/10.6084/m9.figshare.22154576.v1 (91).

Data, Materials, and Software Availability. Code is available online at https://github.com/ignacioq/Tapestree.jl (92). All study data are included in the article and/or supporting information.

ACKNOWLEDGMENTS. We thank Christopher R. Scotese for sharing the palaeogeographic information. We thank Daniele Silvestro, Juan L. Cantalapiedra, and Juan D. Carrillo for help with fossil analyses. We thank Jérémy Andréoletti and the Morlon lab in general for feedback on an earlier draft. We are grateful to the Map of Life team, in particular Yanina Sica and Ajay Ranipeta, for the support in preparing the spatial biodiversity data. This project has received funding from the European Union's Horizon 2020 research and innovation programme under the ERC CoG PANDA to H.M. and Marie Skłodowska-Curie grant agreement No 897225 for I.Q. M.J.L. was supported by NSF-DEB grant 2040347. W.J. acknowledges the support from NSF VertLife grant DEB 1441737.

Author affiliations: [a]Institut de Biologie de l'ENS, Département de Biologie, École Normale Supérieure, CNRS, INSERM, Université Paris Science & Lettres, Paris 75005, France; [b]Landis Lab, Department of Biology, Washington University in St. Louis, St. Louis, MO 63130; [c]Jetz Lab, Department of Ecology and Evolutionary Biology, Yale University, New Haven, CT 06511; and [d]Center for Biodiversity and Global Change, Yale University, New Haven, CT 06511

1. M. Willig, D. Kaufman, R. Stevens, Latitudinal gradients of biodiversity: Pattern, process, scale, and synthesis. *Annu. Rev. Ecol. Evol. Syst.* **34**, 273–309 (2003).
2. K. Rohde, Latitudinal gradients in species diversity: The search for the primary cause. *Oikos* **65**, 514–527 (1992).
3. G. G. Mittelbach *et al.*, Evolution and the latitudinal diversity gradient: Speciation, extinction and biogeography. *Ecol. Lett.* **10**, 315–331 (2007).
4. J. J. Wiens, M. J. Donoghue, Historical biogeography, ecology and species richness. *Trends Ecol. Evol.* **19**, 639–644 (2004).
5. H. Morlon, Diversity hotspots: Coldspots of speciation? *Science* **370**, 1268–1269 (2020).
6. D. Jablonski, K. Roy, J. W. Valentine, Out of the tropics: Evolutionary dynamics of the latitudinal diversity gradient. *Science* **314**, 102–106 (2006).
7. W. Jetz, G. H. Thomas, J. B. Joy, K. Hartmann, A. O. Mooers, The global diversity of birds in space and time. *Nature* **491**, 444–448 (2012).
8. J. Belmaker, W. Jetz, Relative roles of ecological and energetic constraints, diversification rates and region history on global species richness gradients. *Ecol. Lett.* **18**, 563–571 (2015).
9. I. Quintero, W. Jetz, Global elevational diversity and diversification of birds. *Nature* **555**, 246–250 (2018).
10. D. L. Rabosky *et al.*, An inverse latitudinal gradient in speciation rate for marine fishes. *Nature* **559**, 392–395 (2018).
11. J. Igea, A. J. Tanentzap, Angiosperm speciation cools down in the tropics. *Ecol. Lett.* **23**, 692–700 (2020).

12. M. G. Harvey *et al*., The evolution of a tropical biodiversity hotspot. *Science* **370**, 1343–1348 (2020).
13. D. Schluter, M. W. Pennell, Speciation gradients and the distribution of biodiversity. *Nature* **546**, 48–55 (2017).
14. S. A. Fritz *et al*., Diversity in time and space: Wanted dead and alive. *Trends Ecol. Evol.* **28**, 509–516 (2013).
15. A. K. Behrensmeyer, S. M. Kidwell, R. A. Gastaldo, Taphonomy and paleobiology. *Paleobiology* **26**, 103–147 (2000).
16. D. Silvestro *et al*., Fossil biogeography: A new model to infer dispersal, extinction and sampling from palaeontological data. *Philos. Trans. R. Soc. Lond., B, Biol. Sci.* **371**, 20150225 (2016).
17. T. F. Rangel *et al*., Modeling the ecology and evolution of biodiversity: Biogeographical cradles, museums, and graves. *Science* **361**, eaar5452 (2018).
18. O. Hagen, A. Skeels, R. E. Onstein, W. Jetz, L. Pellissier, Earth history events shaped the evolution of uneven biodiversity across tropical moist forests. *Proc. Natl. Acad. Sci. U.S.A.* **118**, e2026347118 (2021).
19. J. M. Beaulieu, B. C. O'Meara, Detecting hidden diversification shifts in models of trait-dependent speciation and extinction. *Syst. Biol.* **65**, 583–601 (2016).
20. D. S. Caetano, B. C. O'Meara, J. M. Beaulieu, Hidden state models improve state-dependent diversification approaches, including biogeographical models. *Evolution* **72**, 2308–2324 (2018).
21. T. Vasconcelos, B. C. O'Meara, J. M. Beaulieu, A flexible method for estimating tip diversification rates across a range of speciation and extinction scenarios. *Evolution* **76**, 1420–1433 (2022).
22. H. E. Beck *et al*., Present and future Köppen–Geiger climate classification maps at 1-km resolution. *Sci. Data* **5**, 180214 (2018).
23. A. H. Hurlbert, W. Jetz, Species richness, hotspots, and the scale dependence of range maps in ecology and conservation. *Proc. Natl. Acad. Sci. U.S.A.* **104**, 13384–13389 (2007).
24. D. L. Rabosky, No substitute for real data: A cautionary note on the use of phylogenies from birth-death polytomy resolvers for downstream comparative analyses. *Evolution* **69**, 3207–3216 (2015).
25. D. Dragomir, E. S. Allman, J. A. Rhodes, Parameter identifiability of a multitype pure-birth model of speciation. *J. Comput. Biol.* **30**, 277–292 (2023).
26. R. A. Pyron, J. J. Wiens, Large-scale phylogenetic analyses reveal the causes of high tropical amphibian diversity. *Proc. R. Soc. B: Biol. Sci.* **280**, 20131622 (2013).
27. J. Rolland, F. L. Condamine, F. Jiguet, H. Morlon, Faster speciation and reduced extinction in the tropics contribute to the mammalian latitudinal diversity gradient. *PLoS Biol.* **12**, e1001775 (2014).
28. P. Pulido-Santacruz, J. T. Weir, Extinction as a driver of avian latitudinal diversity gradients. *Evolution* **70**, 860–872 (2016).
29. J. T. Weir, D. Schluter, The latitudinal gradient in recent speciation and extinction rates of birds and mammals. *Science* **315**, 1574–1576 (2007).
30. D. L. Rabosky, P. O. Title, H. Huang, Minimal effects of latitude on present-day speciation rates in new world birds. *Proc. R. Soc. B: Biol. Sci.* **282**, 20142889 (2015).
31. N. B. Fröbisch, J. C. Olori, R. R. Schoch, F. Witzmann, Amphibian development in the fossil record. *Semin. Cell Dev. Biol.* **21**, 424–431 (2010).
32. T. R. Simoes *et al*., The origin of squamates revealed by a middle Triassic lizard from the Italian Alps. *Nature* **557**, 706–709 (2018).
33. D. J. Field, J. Benito, A. Chen, J. W. Jagt, D. T. Ksepka, Late cretaceous neornithine from Europe illuminates the origins of crown birds. *Nature* **579**, 397–401 (2020).
34. R. B. Benson *et al*., Cretaceous tetrapod fossil record sampling and faunal turnover: Implications for biogeography and the rise of modern clades. *Palaeogeogr. Palaeoclimatol. Palaeoecol.* **372**, 88–107 (2013).
35. R. A. Pyron, Temperate extinction in squamate reptiles and the roots of latitudinal diversity gradients. *Glob. Ecol. Biogeogr.* **23**, 1126–1134 (2014).
36. S. Nee, R. M. May, P. H. Harvey, The reconstructed evolutionary process. *Philos. Trans. R. Soc. Lond., B, Biol. Sci.* **344**, 305–311 (1994).
37. P. D. Mannion, P. Upchurch, R. B. Benson, A. Goswami, The latitudinal biodiversity gradient through deep time. *Trends Ecol. Evol.* **29**, 42–50 (2014).
38. Y. Kisel, T. G. Barraclough, Speciation has a spatial scale that depends on levels of gene flow. *Am. Nat.* **175**, 316–334 (2010).
39. W. Jetz, P. V. A. Fine, Global gradients in vertebrate diversity predicted by historical area-productivity dynamics and contemporary environment. *PLoS Biol.* **10**, 1–11 (2012).
40. A. D. Barnosky, Distinguishing the effects of the red queen and court jester on miocene mammal evolution in the northern rocky mountains. *J. Vertebr. Paleontol.* **21**, 172–185 (2001).
41. J. C. Zachos *et al*., A transient rise in tropical sea surface temperature during the Paleocene–Eocene thermal maximum. *Science* **302**, 1551–1554 (2003).
42. A. P. Allen, J. H. Brown, J. F. Gillooly, Global biodiversity, biochemical kinetics, and the energetic-equivalence rule. *Science* **297**, 1545–1548 (2002).
43. D. L. Rabosky, Diversity-dependence, ecological speciation, and the role of competition in macroevolution. *Annu. Rev. Ecol. Evol. Syst.* **44**, 481–502 (2013).
44. B. C. Emerson, N. Kolm, Species diversity can drive speciation. *Nature* **434**, 1015–1017 (2005).
45. C. R. Scotese, An atlas of phanerozoic paleogeographic maps: The seas come in and the seas go out. *Annu. Rev. Earth Planet. Sci.* **49**, 679–728 (2021).
46. A. Pohl, T. Wong Hearing, A. Franc, P. Sepulchre, C. R. Scotese, Dataset of phanerozoic continental climate and Köppen–Geiger climate classes. *Data Br.* **43**, 108424 (2022).
47. P. V. Fine, R. H. Ree, Evidence for a time-integrated species-area effect on the latitudinal gradient in tree diversity. *Am. Nat.* **168**, 796–804 (2006).
48. S. B. Archibald, W. H. Bossert, D. R. Greenwood, B. D. Farrell, Seasonality, the latitudinal gradient of diversity, and Eocene insects. *Paleobiology* **36**, 374–398 (2010).
49. O. Hagen *et al*., gen3sis: A general engine for eco-evolutionary simulations of the processes that shape earth's biodiversity. *PLoS Biol.* **19**, 1–31 (2021).
50. D. L. Rabosky, I. J. Lovette, Density-dependent diversification in North American wood warblers. *Proc. R. Soc. B: Biol. Sci.* **275**, 2363–2371 (2008).
51. E. Lewitus, H. Morlon, Detecting environment-dependent diversification from phylogenies: A simulation study and some empirical illustrations. *Syst. Biol.* **67**, 576–593 (2018).
52. S. Louca, M. W. Pennell, Extant timetrees are consistent with a myriad of diversification histories. *Nature* **580**, 502–505 (2020).
53. T. W. Davies, M. A. Bell, A. Goswami, T. J. D. Halliday, Completeness of the eutherian mammal fossil record and implications for reconstructing mammal evolution through the Cretaceous/Paleogene mass extinction. *Paleobiology* **43**, 521–536 (2017).
54. J. D. Archibald, The importance of phylogenetic analysis for the assessment of species turnover: A case history of Paleocene mammals in North America. *Paleobiology* **19**, 1–27 (1993).
55. D. Silvestro, R. Warnock, A. Gavryushkina, T. Stadler, Closing the gap between palaeontological and neontological speciation and extinction rate estimates. *Nat. Commun.* **9**, 1–14 (2018).
56. E. E. Saupe *et al*., Climatic shifts drove major contractions in avian latitudinal distributions throughout the cenozoic. *Proc. Natl. Acad. Sci. U.S.A.* **116**, 12895–12900 (2019).
57. W. Jetz, R. A. Pyron, The interplay of past diversification and evolutionary isolation with present imperilment across the amphibian tree of life. *Nat. Ecol. Evol.* **2**, 850–858 (2018).
58. J. F. R. Tonini, K. H. Beard, R. B. Ferreira, W. Jetz, R. A. Pyron, Fully-sampled phylogenies of squamates reveal evolutionary patterns in threat status. *Biol. Conserv.* **204**, 23–31 (2016).
59. N. S. Upham, J. A. Esselstyn, W. Jetz, Inferring the mammal tree: Species-level sets of phylogenies for questions in ecology, evolution, and conservation. *PLoS Biol.* **17**, e3000494 (2019).
60. H. B. Lillywhite, C. M. Sheehy, F. Brischoux, A. Grech, Pelagic sea snakes dehydrate at sea. *Proc. R. Soc. B: Biol. Sci.* **281**, 20140119 (2014).
61. F. Brischoux, R. Tingley, R. Shine, H. B. Lillywhite, Salinity influences the distribution of marine snakes: Implications for evolutionary transitions to marine life. *Ecography* **35**, 994–1003 (2012).
62. IU for Conservation of Nature, The IUCN red list of threatened species. https://www.iucnredlist.org/ (2016). Accessed 1 January 2018.
63. U. Roll *et al*., The global distribution of tetrapods reveals a need for targeted reptile conservation. *Nat. Ecol. Evol.* **1**, 1677–1682 (2017).
64. D. M. C. C. Alves, J. A. F. Diniz-Filho, F. Villalobos, Geographical diversification and the effect of model and data inadequacies: The bat diversity gradient as a case study. *Biol. J. Linn. Soc.* **121**, 894–906 (2017).
65. O. Maliet, F. Hartig, H. Morlon, A model with many small shifts for estimating species-specific diversification rates. *Nat. Ecol. Evol.* **3**, 1086–1092 (2019).
66. O. Maliet, H. Morlon, Fast and accurate estimation of species-specific diversification rates using data augmentation. *Syst. Biol.* **71**, 353–366 (2022).
67. A. Gelman, D. B. Rubin, Inference from iterative simulation using multiple sequences. *Stat. Sci.* **7**, 457–472 (1992).
68. J. D. Hadfield, Mcmc methods for multi-response generalized linear mixed models: The MCMCglmm R package. *J. Stat. Softw.* **33**, 1–22 (2010).
69. R Core Team, *R: A Language and Environment for Statistical Computing* (R Foundation for Statistical Computing, Vienna, Austria, 2020).
70. GDAL/OGR contributors, *GDAL/OGR Geospatial Data Abstraction software Library* (Open Source Geospatial Foundation, 2020).
71. R. J. Hijmans, *raster: Geographic Data Analysis and Modeling* (R Package Version 2.9-23, 2019).
72. F. L. Condamine, J. Rolland, H. Morlon, Assessing the causes of diversification slowdowns: Temperature-dependent and diversity-dependent models receive equivalent support. *Ecol. Lett.* **22**, 1900–1912 (2019).
73. J. Ramsey, B. Ripley, *pspline: Penalized Smoothing Splines* (R Package Version 1.0-18, 2017).
74. J. L. Cantalapiedra *et al*., Dietary innovations spurred the diversification of ruminants during the caenozoic. *Proc. R. Soc. B: Biol. Sci.* **281**, 20132746 (2014).
75. R. G. FitzJohn, Diversitree: Comparative phylogenetic analyses of diversification in R. *Methods Ecol. Evol.* **3**, 1084–1092 (2012).
76. E. E. Goldberg, L. T. Lancaster, R. H. Ree, Phylogenetic inference of reciprocal effects between geographic range evolution and diversification. *Syst. Biol.* **60**, 451–465 (2011).
77. J. Barido-Sottani, T. G. Vaughan, T. Stadler, A multitype birth–death model for Bayesian inference of lineage-specific birth and death rates. *Syst. Biol.* **69**, 973–986 (2020).
78. M. J. Landis, I. Quintero, M. M. Muñoz, F. Zapata, M. J. Donoghue, Phylogenetic inference of where species spread or split across barriers. *Proc. Natl. Acad. Sci. U.S.A.* **119**, e2116948119 (2022).
79. D. R. Cox, Regression models and life-tables. *J. R. Stat. Soc., B: Stat. Methodol.* **34**, 187–202 (1972).
80. I. Quintero, M. J. Landis, Interdependent phenotypic and biogeographic evolution driven by biotic interactions. *Syst. Biol.* **69**, 739–755 (2020).
81. H. Morlon *et al*., Rpanda: An R package for macroevolutionary analyses on phylogenetic trees. *Methods Ecol. Evol.* **7**, 589–597 (2016).
82. J. Bezanson, A. Edelman, S. Karpinski, V. B. Shah, Julia: A fresh approach to numerical computing. *SIAM Rev.* **59**, 65–98 (2017).
83. C. Rackauckas, Q. Nie, Differentialequations.jl–A performant and feature-rich ecosystem for solving differential equations in Julia. *J. Open Res. Software* **5**, 15 (2017).
84. G. Altekar, S. Dwarkadas, J. P. Huelsenbeck, F. Ronquist, Parallel metropolis coupled Markov chain Monte Carlo for Bayesian phylogenetic inference. *Bioinformatics* **20**, 407–415 (2004).
85. N. Goldman, Simple diagnostic statistical tests of models for DNA substitution. *J. Mol. Evol.* **37**, 650–661 (1993).
86. S. Duchene, R. Bouckaert, D. A. Duchene, T. Stadler, A. J. Drummond, Phylodynamic model adequacy using posterior predictive simulations. *Syst. Biol.* **68**, 358–364 (2018).
87. TP Database, The data were downloaded from the paleobiology database (paleobiodb.org) on July, 2022, using the group name 'Mammalia' (2022).
88. J. J. Sepkoski, Rates of speciation in the fossil record. *Philos. Trans. R. Soc. Lond., B, Biol. Sci.* **353**, 315–326 (1998).
89. D. Jablonski, J. A. Finarelli, Congruence of morphologically-defined genera with molecular phylogenies. *Proc. Natl. Acad. Sci. U.S.A.* **106**, 8262–8266 (2009).
90. W. Köppen, Die wärmezonen der erde, nach der dauer der heissen, gemässigten und kalten zeit und nach der wirkung der wärme auf die organische welt betrachtet. *Meteorol. Z.* **1**, 5–226 (1884).
91. I. Quintero, SI Appendix for The build-up of the present-day tropical diversity of tetrapods. Figshare. https://doi.org/10.6084/m9.figshare.22154576.v1. Deposited 24 April 2023.
92. I. Quintero, Tapestree. GitHub. https://github.com/ignacioq/Tapestree.jl. Deposited 26 October 2022.